



A Review of the Principles and Applications of Seismic Methods in Geophysical Prospecting with OpendTect in focus

Tsepav, M.T.

Department of Physics, Ibrahim Badamasi Babangida University, Lapai, Nigeria

ABSTRACT

Seismic methods are increasingly becoming the most reliable and efficient of all geophysical methods in studying the subsurface due to their higher resolution and flexibility in interpretation. The advancement in technology, culminating in the development of interpretation software has made seismic data interpretation very interesting with a commendable degree of accuracy. It is therefore, imperative to review some of the seismic methods that are mostly used in prospecting for minerals and other subsurface structures of geological and geophysical interest. In this review, we bring to fore the basic principles and applications of refraction and reflection seismic methods and elucidate how one of the most recent and proficient interpretation software for seismic data interpretation, the OpendTect could be used for interpretation of seismic data.

Keywords: Reflection, Refraction, Seismic, Exploration, OpendTect.

INTRODUCTION

Seismic exploration involves surveying subterranean geological formations for hydrocarbon deposits. A survey typically involves deploying seismic source(s) and seismic sensors at predetermined locations. The sources generate seismic waves, which propagate into the geological formations creating pressure changes and vibrations along their way. Changes in elastic properties of the geological formation scatter the seismic waves, changing their direction of propagation and other properties. Part of the energy emitted by the sources reaches the seismic sensors. Some seismic sensors are sensitive to pressure changes (hydrophones), others to particle motion (e.g., geophones), and industrial surveys may deploy only one type of sensor, both hydrophones and geophones, and/or other suitable sensor types (Everhard *et al.*, 2015).

Seismic methods make use of the fact that elastic waves travel with different velocities in different rock types. The basic principle is to initiate such waves at a point and determine at some other point the arrival time of the energy that is refracted or reflected by the discontinuities between different

rock formations. This then enables the position of the discontinuities to be detected.

The standard technique for producing seismic waves is to detonate dynamites in a drilled hole and observe the arrival time on a set of geophones mounted at intervals from the shot point. The data obtained leads to almost unique and unambiguous interpretation, if properly handled.

Seismic prospecting is based on the theory of elasticity. Elastic moduli describe the physical properties of the rock and determine the seismic velocity. The elastic properties of a substance are characterized by elastic moduli or constant which specify the relationship between stress and strain (Parasnis, 1979). According to Hooke's law, if F is stress, χ the strain and k the elastic constant, then these parameters can be represented by:

$$F = k\chi \quad (1)$$

There are two moduli of great importance in the study of elastic waves in the earth: Bulk modulus

Received 15 June, 2022

Accepted 23 August, 2022

Address Correspondence to:

tsematoo@yahoo.com

Tsepav, 2022

and shear modulus, defined respectively as:

$$\text{Shear modulus, } \mu = \frac{\text{Shear stress}}{\text{Shear strain}}$$

$$\text{Bulk modulus, } \kappa = \frac{\text{Volume stress}}{\text{Volume strain}}$$

Table 1: The range of values for bulk and shear moduli for different substances

Substance	Marble/ limestone	Granite	Sandstone	Wrought iron	Cast iron	Crown glass	Fiber quartz
Bulk modulus (K)	3.7 - 5.7	2.7 - 3.3	1.25	16.00	9.50	5.00	1.50
Shear modulus (μ)	2.1 - 3.0	1.5 - 2.4	0.61	7.70	5.00	2.50	3.00

Table 1 shows the values for bulk and shear moduli for different substances. From these values, one could have an idea of the primary V_p and secondary velocities, V_s through equations (2) and (3) respectively, if the density ρ of the medium is known.

$$V_p = \left[\frac{K + \frac{4}{3}\mu}{\rho} \right]^{\frac{1}{2}} \quad (2)$$

$$V_s = \left(\frac{\mu}{\rho} \right)^{\frac{1}{2}} \quad (3)$$

The velocities are generally greater in crystalline rocks than in sedimentary rocks. In Sedimentary rocks, velocities tend to increase with depth of burial and geologic age. It has been shown (Parasnis, 1979) that for shale and sand:

$$V = 46.5 (Z T)^{\frac{1}{6}} \text{ m/s} \quad (4)$$

where Z = depth of burial and T = time in years.

Seismic Refraction and Reflection Theories

Seismic Refraction Method

Most applications of explosion seismology in the investigation of crustal layering and thickness make use of the refraction method of seismic prospecting. The basic idea is to determine the travel time of primary waves between shot points and geophones at varying distances apart (Parasnis, 1979).

Two layer earth model

If we consider a situation where a layer in which the waves have a velocity, V_1 is underlain by another layer of velocity, V_2 , then according to Snell's law:

$$\frac{V_1}{V_2} = \frac{\sin i_1}{\sin i_2} \quad (5)$$

where i_1 and i_2 are the angles of incidence and refraction for the seismic wave as shown in Figure 1.

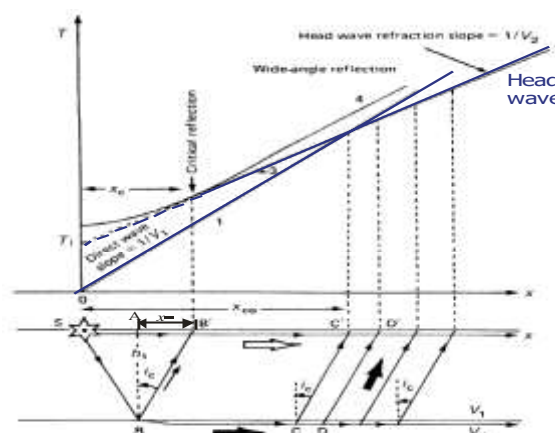


Figure 1: Time – distance graph of the refractive seismic method for a two – layer model

In Figure 1, the direct waves, critically refracted waves, late refracted arrivals and reflected waves are represented by numbers 1 to 4 respectively. The critically reflected waves start arriving after

Tsepav, 2022

critical distance x_c , but they overtake the direct waves at a cross over distance x_{co} .

From the diagram, the ray SB with the critical angle of incidence $i_1 = i_c$ is refracted so that $i_2 = 90^\circ$ and travels along the boundary between the two media. Hence from equation (5)

$$\frac{\sin i_c}{\sin 90^\circ} = \frac{V_1}{V_2}$$

$$\Rightarrow \sin i_c = \frac{V_1}{V_2} \quad (6)$$

This equation holds only for $V_2 > V_1$. This ray subjects the interface to oscillatory stress and each point on it sends out secondary waves and waves such as CC' emerge on the surface at an angle i_c to reach the geophone.

If the geophone is near the shot point, S (assumed to be on the surface), direct waves arrive at the geophone first along SC' before the arrival of the refracted wave. If on the other hand, the distance SC' is sufficiently great, the refracted wave $SBCC'$ arrives first. It overtakes the direct wave because of the higher velocity along the path BC. The travel time for direct wave is given by

$$t = \frac{x}{V_1} \quad (7)$$

A plot of t vs x gives $\frac{1}{V_1}$ as slope.

The travel time for the refracted wave is given by

$$t = \frac{SB}{V_1} + \frac{BC}{V_2} + \frac{CC'}{V_1} \quad (8)$$

If we assume horizontally parallel layering then $SB = CC'$

$$\Rightarrow t = \frac{2SB}{V_1} + \frac{BC}{V_2} \quad (9)$$

If we consider triangle ABB' in Figure 1, then

$$\sin i_c = \frac{x}{BB'} \quad (10)$$

$$\text{But } (BB')^2 = h_1^2 + x^2 \quad (11)$$

From equation (6) and (10)

$$x = BB' \frac{V_1}{V_2} \quad (12)$$

Putting equation (12) into (11) yields:

$$(BB')^2 = h_1^2 + (BB')^2 \frac{V_1^2}{V_2^2}$$

$$\Rightarrow BB' = \frac{h_1 V_2}{(V_2^2 - V_1^2)^{\frac{1}{2}}} = SB \quad (13)$$

$$\text{Also } BC = x_{co} - 2x \quad (14)$$

$$\text{From } \tan i_c = \frac{\sin i_c}{\cos i_c} = \frac{x}{h_1}$$

$$\Rightarrow \frac{x}{h_1} = \frac{V_1/V_2}{(V_2^2 - V_1^2)^{\frac{1}{2}}/V_2} = \frac{V_1}{(V_2^2 - V_1^2)^{\frac{1}{2}}}$$

$$(\cos i_c = \frac{h_1}{BB'})$$

$$\Rightarrow x = \frac{h_1 V_1}{(V_2^2 - V_1^2)^{\frac{1}{2}}} \quad (15)$$

Using (13), (14) and (15) in (9) we get

$$t = \frac{2h_1 V_2}{V_1 (V_2^2 - V_1^2)^{\frac{1}{2}}} + \frac{x_{co}}{V_2} - \frac{\left(\frac{2h_1 V_1}{V_2}\right)}{(V_2^2 - V_1^2)^{\frac{1}{2}}}$$

$$= 2h_1 \left[\frac{V_2}{V_1 (V_2^2 - V_1^2)^{\frac{1}{2}}} - \frac{V_1}{V_2 (V_2^2 - V_1^2)^{\frac{1}{2}}} \right] + \frac{x}{V_2}$$

$$= 2h_1 \left[\frac{(V_2^2 - V_1^2)}{V_1 V_2 (V_2^2 - V_1^2)^{\frac{1}{2}}} \right] + \frac{x}{V_2}$$

$$\therefore t = \frac{2h_1 (V_2^2 - V_1^2)^{\frac{1}{2}}}{V_1 V_2} + \frac{x}{V_2} \quad (16)$$

\Rightarrow a plot of t against x is a straight line graph with slope $= \frac{1}{V_2}$ and intercept on the t - axis given by:

$$t_i = \frac{2h_1 (V_2^2 - V_1^2)^{\frac{1}{2}}}{V_1 V_2} \quad (17)$$

equation (17) is called the delay time

Since $\cos^2 \theta + \sin^2 \theta = 1$

$$\cos i_c = \frac{(V_2^2 - V_1^2)^{\frac{1}{2}}}{V_2}$$

$$\Rightarrow t_1 = \frac{2h_1}{V_1} \cos i_c \quad (18)$$

Tsepav, 2022

When direct waves and refracted waves arrive the geophone at the same time:

$$\begin{aligned} \frac{x}{V_1} &= \frac{x}{V_2} + \frac{2h_1(V_2^2 - V_1^2)^{1/2}}{V_1V_2} \\ \Rightarrow x \left(\frac{1}{V_1} - \frac{1}{V_2} \right) &= \frac{2h_1(V_2^2 - V_1^2)^{1/2}}{V_1V_2} \\ \Rightarrow x \frac{(V_2 - V_1)}{V_1V_2} &= \frac{2h_1(V_2^2 - V_1^2)^{1/2}}{V_1V_2} \\ \Rightarrow x &= \frac{2h_1(V_2^2 - V_1^2)^{1/2}}{V_2 - V_1} \\ &= \frac{2h_1[(V_2 - V_1)(V_2 + V_1)]^{1/2}}{(V_2 - V_1)} \\ x_c &= 2h_1 \left(\frac{V_2 + V_1}{V_2 - V_1} \right)^{1/2} \end{aligned} \quad (19)$$

x_c is called the critical distance which is the distance at which both the direct and refracted waves arrive the detectors at the same time. Beyond this distance, the refracted waves arrive first at the geophones. It is therefore evident that a time – distance graph of the first arrivals at the geophone planted at various distances from the shot point will show two intersecting straight lines whose slopes give V_1 and V_2 (Figure 1). The point of intersection, x_c yields the thickness, h_1 of the top layer which is the parameter of interest. From equation (19),

$$h_1 = \frac{x_c}{2 \left(\frac{V_2 + V_1}{V_2 - V_1} \right)^{1/2}} \quad (20)$$

Alternatively, h_1 may be determined from the intercept, t , on the t – axis of equation (15) as expressed in equation (16).

i.e. $h_1 = \frac{V_1 t_1}{2 \cos i_c}$

Three layered Earth Model

The same mathematical analysis as used for a two layer model applies to the three layer earth. Figure 2 illustrates the scenario in a three layer earth model. In this case:

$$Travel\ time, T_{SG} = \frac{SA}{V_1} + \frac{AB}{V_2} + \frac{BC}{V_3} + \frac{CD}{V_2} + \frac{DG}{V_1} \quad (21)$$

$$T_{SG} = \frac{2z_1}{V_1 \cos \theta_1} + \frac{2z_2}{V_2 \cos \theta_c} + \frac{x - 2z_1 \tan \theta_1 - 2z_2 \tan \theta_c}{V_3} \quad (22)$$

This yields

$$T_{SG} = \frac{x}{V_3} + \frac{2z_1 \sqrt{V_3^2 - V_1^2}}{V_3 V_1} + \frac{2z_2 \sqrt{V_3^2 - V_2^2}}{V_3 V_2} \quad (23)$$

From equation (23) we can determine V_1 , V_2 and V_3 from slopes; z_1 from the first intercept and z_2 from the second intercept as shown in Figure 3.

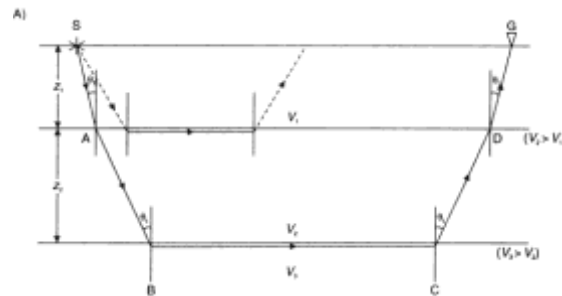


Figure 2: Three layer Earth model

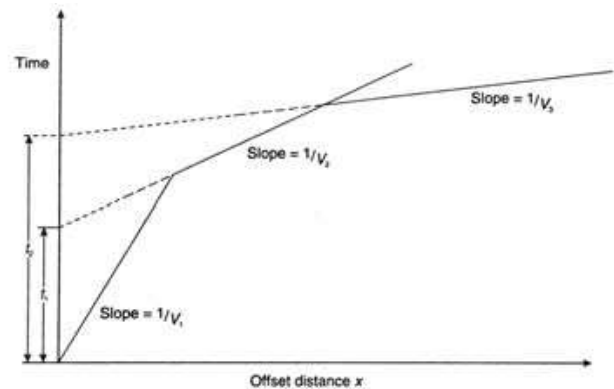


Figure 3a: Time – Distance graph for a three-layer earth model

Seismic Reflection Method

The depth to an interface between two rock formations can be determined by measuring the travel time of a seismic wave generated at the surface and reflected back from the interface. The assumption in reflection seismic is that the observed reflections are only P-P reflection.

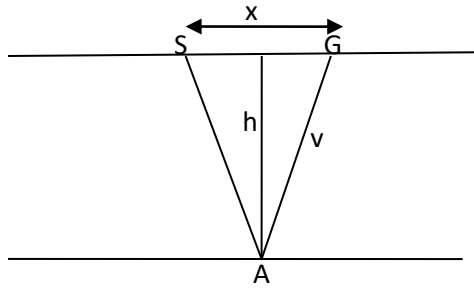


Figure 3b: Seismic reflection

If V is the uniform velocity above the reflecting horizon, then from Figure 3:

$$(SA)^2 = \frac{x^2}{4} + h^2 = (AG)^2 \quad (24)$$

The total distance from S through A to G is then $SAG = SA + AG = 2SA = 2AG$

$$= 2\sqrt{\frac{x^2}{4} + h^2}$$

$$\therefore t = \frac{2}{V}\sqrt{\frac{x^2}{4} + h^2} \quad (25)$$

$$\Rightarrow h = \frac{1}{2}\sqrt{t^2 V^2 - x^2} \quad (26)$$

Either of equations (b) or (c) shows that the $x - t$ curve is a hyperbola convex towards the $x -$ axis and with the $t -$ axis as the symmetry with the line through $x = 0, t = 0$ is its asymptote as shown in Figure 4.

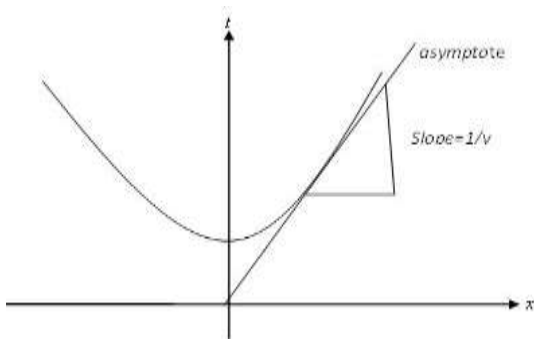


Figure 4: Time -Distance curve for Reflection Seismic

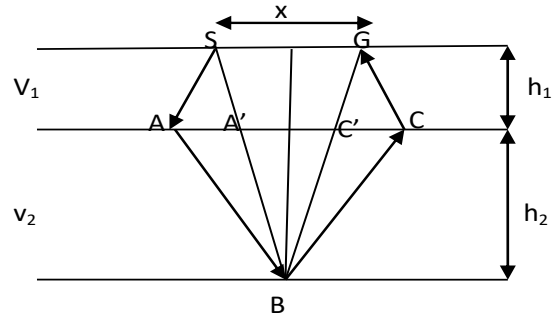


Figure 5: Two – layer reflection model

Figure 5 consists of the refracted wave $SABCG$ and a reflected wave $SA'BC'G$. If the detector distances are very short, $SABCG$ will be neglected, leaving $SA'BC'G$. For a strictly vertical ray,

$$t = \frac{h_1}{v_1} + \frac{h_2}{v_2} = \frac{h_1 + h_2}{\bar{v}} \quad (27)$$

where \bar{v} is the formation velocity over the penetration.

If ρ_1 and ρ_2 represent the densities of the first and second layers respectively and A_0, A_1 and A_2 represent the amplitudes of the incident, transmitted and reflected waves respectively, then we define the reflection coefficient:

$$R = \frac{A_1}{A_0} = \frac{\rho_2 v_2 - \rho_1 v_1}{\rho_2 v_2 + \rho_1 v_1} = \frac{Z_2 - Z_1}{Z_1 + Z_2} \quad (28)$$

where $z = \rho V$ is the acoustic impedance.

The transmission coefficient

$$T = \frac{A_2}{A_0} = \frac{2\rho_1 v_1}{\rho_2 v_2 + \rho_1 v_1} \quad (29)$$

It is to be noted here, that $-1 \leq R \leq 1$.

- a) If $R = 0, Z_1 = Z_2$ and all incident energy is transmitted and there is no reflection
- b) If $R = -1$ or 1 , all incident energy is reflected
- c) If $R < 0$, there is a phase change of 180° in reflected wave.

For a multilayer earth model, the formation velocity is given by

Tsepav, 2022

$$\bar{v} = \frac{\sum_{j=1}^n h_j}{\sum_{j=1}^n \left(\frac{h_j}{v_j}\right)} = \frac{\text{total distance}}{\text{total time}} \quad (30)$$

Although seismic reflection has a better resolution than seismic refraction, the former is more expensive.

Table 2 shows a comparative description of Seismic Reflection and Seismic Refraction.

In situations where both can be applied, seismic reflection generally has a better resolution but is considerably more expensive

Comparison between Seismic methods

Table 2: Comparison between Seismic Reflection and Seismic Refraction

	Seismic Methods	
	Refraction	Reflection
Typical Targets	Near-horizontal density contrast at depths less than ~100feet	Horizontal to dipping density contrast and laterally restricted targets such as cavities or tunnels at depths greater than ~50 feet.
Required Site Conditions	Accessible dimensions greater than ~5x the depth of interest; unpaved greatly preferred.	None
Vertical Resolution	10 to 20 percent of depth.	5 to 10 percent of depth.
Lateral Resolution	~1/2 the geophone spacing	~1/2 the geophone spacing
Effective Practical Survey Depth	1/5 to 1/4 the maximum shot – geophone separation	>50 feet
Relative Cost	N x	N 3x to N 5x

Seismic Pulse

Simple ray diagrams have been used in the development of seismic theories with the assumption that the horizon is a flat horizontal surface (Červený et al, 2007). This however, does not give a complete physical description of the seismic phenomenon as the horizon is ideally an undulating surface. In actual fact, when a charge is detonated, the material around it is permanently distorted and a cavity is formed while earth ward travelling seismic impulses are generated. Even at distances as large as a couple of meters from the charge, the maximum stress experienced by the material may exceed the range of reversible stress – strain relationship. The distance around the shot point at which the maximum stress falls within this relationship defines the *equivalent cavity* (Brenett, 2009). This region, rather than the shot itself is regarded as the source of seismic wave.

Apart from some large velocity contrasts that cause strong reflections, there are a number of minor velocity contrasts in a geologic column. Each of these, as well as other inhomogeneities will initiate a reflection pulse which arrives on the surface in a broaden form. Therefore, the seismic record between two strong reflections consists, not merely of noise, but to a large extent such reflections superimposed on interfering with one another.

Seismic Data Acquisition

Seismic data can be obtained on land, in air or in the marine environment. Different approaches are therefore used in data acquisition based on where the data is obtained.

Land Seismic Data Acquisition

The first thing to do is to clear the area of investigation. The area is then surveyed to determine shot and receiver locations using integrated handheld survey equipment which uses GPS to determine distances, elevations, and locations. Shot holes are then drilled if dynamites are the sources of energy. The geophones are then firmly planted on the ground in a straight line through the points on the surface vertically above the shot points (Figure 6) or arranged in a circular form (fan shooting) and then connected to recording equipment through long cables. Flags are planted at shot and receiver-station locations. When the amplifier gain and filters are appropriately set and the recording film is set in motion, the shot is fired. The recording is stopped after a few seconds when the ground motion must have subsided.

After the shot-holes or vibrating points are recorded, cables are moved to the adjoining area to continue the survey. Moving cables should be properly coordinated with data acquisition and movement of equipment and personnel should not interfere with data recording. Data acquisition in the vicinity of cultural locations should be coordinated to increase safety and decrease noise.

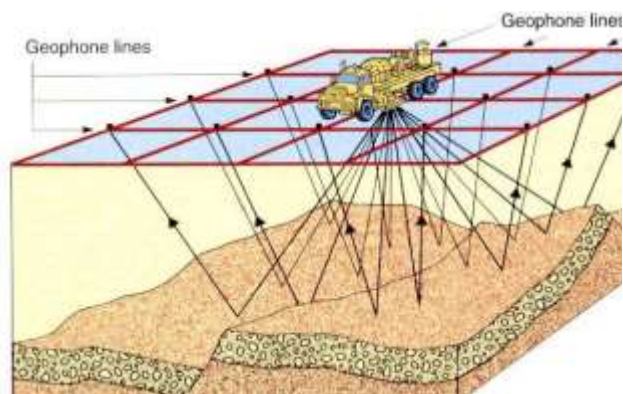


Figure 6: Land Seismic Data Acquisition set up

Airborne Seismic Data Acquisition

This involves the use of unmanned airborne vehicle which is equipped with a seismic sensor and is adapted to fly to a position to deploy the

sensor as an acquisition point of the seismic acquisition system. The flying of this unmanned airborne vehicle in proximity to a seismic acquisition network makes it possible to communicate with at least one node of the seismic acquisition network. In response to the detected seismic events, the sensors generate electrical signals to produce seismic data. Analysis of the seismic data can then indicate the presence or absence of probable locations of minerals of economic interest.

Marine Seismic Data Acquisition

In a marine operation, a ship tows one or more energy sources fastened parallel with one or more towed seismic receiver lines. In this case, the receiver lines take the form of cable called Steamer containing a number of hydrophones (Talagapu, 2017). The vessel moves along and fires a shot, with reflections recorded by the streamers. If a single streamer and a single source are used, a single seismic profile may be recorded in like manner to the land operation. If a number of parallel sources and/or streamers are towed at the same time, the result is a number of parallel lines recorded at the same time. If many closely spaced parallel lines are recorded, a 3D data volume is recorded (Talagapu, 2017). More than one vessel may be employed to acquire data on 24-hour basis, since there is no need to curtail operations in nights.

Seismographs

The seismic records obtained consist of wiggles (wave like disturbances). The wiggles on a single trace may represent reflected pulse or ground movement due to noise (caused by wind or ground roll) and there will be no way of distinguishing a signal if only one trace is present.

However, if there are many traces present, the noise traces are unlikely to be exactly in phase at all geophones, but a true pulse reflected from a lithologic surface arrives at the various geophones approximately at the same time as the geophones are close to one another. The reflections are therefore recognized by the lining

Tsepav, 2022

–up of the crests and troughs on the adjacent traces across the entire record. This lining –up is almost straight for later reflection but for earlier reflections, the pulses lie on a slightly curved line called a hyperbola. The normal move outs (nmos) are calculated from the knowledge of average velocity \bar{V} . If this correction is done and the pulses continue to show step outs in arrival times, then the interface might be a dipping type.

Minerals Exploration

While the seismic reflection methods used for petroleum and minerals exploration are similar, mineral exploration poses special problems that must be taken into account. Most economic mineral deposits are found in hard rock, rather than sedimentary environments. Since the impedance contrasts and reflection coefficients between most common igneous and metamorphic rocks are smaller than those between sedimentary rocks ($R \sim 0.1$ vs. 0.3), the signal-to-noise (S/N) ratio in minerals surveys will be low, making it more difficult to image structures in the country rock (Eaton *et al.*, 2003). Particular care must thus be taken during acquisition and processing to maximize the S/N ratio. This is typically done by using explosives in shallow boreholes filled with water or tamped with sand to ensure good source coupling to bedrock, by using cemented or clamped geophones whenever possible, by careful testing of different sources before conducting the survey itself, and by maximizing the fold (Eaton *et al.*, 2003).

Velocities in igneous and metamorphic rocks are typically higher than sediments. Since wavelength varies with velocity for any given frequency, higher frequencies are required in hard rocks than sediments to achieve comparable resolution, which is another reason for using explosives. Structures in hard rock terrains are often complex and steeply dipping, requiring high resolution (>100 Hz), high fold surveys to be resolved (Salisbury and Snyder, 2007). Since reflections from dipping reflectors tend to arrive at the surface at unexpected locations, it is often necessary to model surveys in such terrains in advance in order to determine

the optimum locations for receivers and to interpret the data. Since even rich ore deposits are often fairly small (<1 km across), they commonly appear as diffractions rather than reflections on seismic reflection profiles. Processing of reflection data from mineral surveys thus often involves two processing streams, one to image structures such as folds or faults in country rock and to locate, enhance, and trace diffractions to their sources using unmigrated data.

Prestack migration, a sophisticated processing technique in which the data is migrated without any prior stacking, is used in this second stream because conventional processing tends to treat small targets as noise. Since some types of ores only have small impedance contrasts with many common host rocks, it is often advisable to conduct laboratory measurements of the velocities and densities of the ores and host rocks in a potential survey area to determine whether reflections are even possible and the survey worth conducting.

Seismic Data Processing

After shooting, the geophone data is multiplexed and transmitted back to a central field computer where it is preprocessed and recorded for subsequent digital processing to remove noise and present the data as a geometrically correct plot of reflection amplitude versus time (depth) and distance along the seismic line (Yilmaz, 1987). Preprocessing in the field involves demultiplexing and reformatting the data from the receiver array. Environmental noise has to be edited out and amplitude adjustments, such as automatic gain control (AGC), need to be applied to correct for geometric spreading. In addition, the geometry of the survey (latitude, longitude, and elevation of shot and receiver positions) is established at this time and initial static corrections (time shifts) are applied to the data based on the geometry.

After preprocessing, the data is simplified by deconvolving all but the initial wavelet of the source signal from the received signal and all of the signals received from each common depth or

Tsepav, 2022

midpoint (CMP) along the line are gathered. Velocities are then estimated as a function of time (velocity analysis) for selected CMP gathers by determining the velocity that best flattens the gather at each depth. This allows the static corrections to be improved by incorporating the effects of shallow low-velocity zones caused by weathering, which in turn, allows for reiterative improvement of the velocity analyses themselves. Once this is done, the signals are further improved by stacking the flattened gathers (i.e. applying the normal moveout, or NMO correction) for each reflection point (bin) to improve the signal-to-noise ratio. The degree of improvement increasing with the square root of the number (fold) of shot-receiver pairs that are stacked for each CMP. Time-variant band pass filters are then applied to normalize the signal for attenuation effects and to examine the data at selected frequencies, and finally, the data is migrated to restore the geometry and the results adjusted for strike and crooked line effects. Finally, the reflection data is presented as a function of depth. All of the processing steps outlined above are conducted in the time domain.

Filtering Technique

The objective of filtering is to eliminate noise. This noise is mainly due to the surface wave referred to a ground roll, and wind. The usual practice is to cut off the low frequencies associated with ground roll with a high pass filter. The filter distorts the shape of the signal (i.e. it could lengthen the signal or shift it). Subsequently, filters create interference patterns on a seismogram in addition to those created by signals.

Another method used to minimize noise in seismic method is the use of multiple geophone arrays. Here, the geophones are laid out along profiles having close spacing of about 10m apart. The outputs of several adjacent geophones are added and recorded as a single trace. If the geophone groups are appropriately selected, the instantaneous motion of the ground due to the vertical component of the surface wave will be upward on some geophones and down ward on

others, So that the sum of the output will eliminate surface waves from the records.

Deconvolution - The seismic convolutional model states that a seismic record is the convolution of the earth's reflectivity with the seismic wavelet. In seismic processing the purpose of deconvolution is to remove (or collapse) the seismic wavelet. In this way, the deconvolved seismic record provides an estimate of the reflectivity. Deconvolution is usually described in terms of the appearance of the deconvolved seismic record, as to whether the events have their durations significantly shortened or not.

Interpretation of Seismic Data

The first step is to calculate the normal move outs (nmos). The nmos is the correction effected on the data to reduce the effects of the non – vertical rays. This is possible with the use of the information on the formation velocity, \bar{V} .

After nmos correction, there should be no step outs in arrival time except where the reflecting horizon is dipping. Once the reflection time is identified on a seismograph and the value of the formation velocity is known, the rest of the interpretation is straight forward. The depth to the reflecting horizon is read – off some convenient monogram based on the expression:

$$h = \frac{1}{2}(V^2t^2 - x^2)^{1/2} \quad (31)$$

It is then plotted midway between the shots and the detector on a diagram representing the vertical cross – section through the shooting profile. However, certain corrections (static and dynamic) must be applied to the observed travel time.

In another method of computing this depth, the reflection times are scaled off the seismograph and plotted directly on a cross – section map. The depths are then obtained by converting the times by means of the distribution of velocity assigning depths to reflecting horizon or selected events on the bases of presumed \bar{V} values called *migration*. The process of selecting reflection time and migration is done automatically.

Tsepav, 2022

Determination of Depth to Reflector/Refractor

Information on formation velocity and arrival time is needed to determine the depth to the reflection/refraction surface (Heubschera and Gohl, 2014). It is usual to apply two corrections to the observed travel times of seismic waves: for elevation differences and for weathering.

The theory assumes that both the shot points and detectors are at the same level, but in general, these elevations differ. It is customary to reduce the arrival time by projecting the shots and detector on to a common horizontal datum plane as shown in Figure 7. Methods of determining formation velocity include Surface method, Sub-Surface method and Laboratory method.

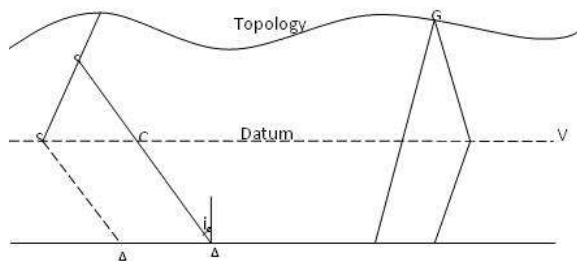


Figure 7: correction to arrival time

OpendTect

OpendTect is a seismic post-processing and interpretation system, as well as a research and development platform for developing innovative seismic interpretation tools (OpendTech, 2010). Workflows for horizon tracking, fault interpretation, drawing of polygons and bodies etc. have been adapted to benefit from the superior hand-eye co-ordination offered by the pen device.

The system features:

- Visualization and analysis of 2D and 3D seismic data in a single survey.
- Sophisticated 2D and 3D horizon tracking including auto-tracking, plane-by-plane, line and manual tracking.
- On-the-fly calculation and visualization of various attributes and filters.

- Multi-platform distributed computing
- Plug-in architecture.

OpendTect can be used amongst others:

- To do seismic data interpretation.
- To create advanced single-attribute cubes.
- To filter the seismic data.
- To track and filter horizons
- To combine attribute and filter responses by math and logic (IF..THEN..ELSE, ..AND.., ..OR.. etc.)
- As a platform to develop new applications or plug-ins.

Projects in OpendTect are associated with a *seismic survey*, which must be defined at the start. The survey specifications define the geographical boundaries of the study area and the relationship between inline/cross-line and X/Y co-ordinate system. Seismic data is loaded from external sources (e.g. SEG Y) into OpendTect's CBVS (Common Binary Volume Storage) format. In using OpendTect, the following terminologies are imminent.

Attribute: An attribute is a derived quantity from a seismic input set. They are defined by a name, a value, and a position in 3D space (inline, cross-line and Z (2WT or depth)). Attributes can be calculated from single-trace, multi-trace, and multi-volume inputs. They can be steered and/or chained. Steered attributes are multi-trace attributes in which the trace segments are found by following a (pre-) calculated dip-azimuth. Chained attributes are attributes derived from other attributes. For example, Similarity and Energy are separate attributes that can be chained to calculate the Similarity of the Energy using the "Position" attribute.

Body: A body is an element that defines an arbitrary three dimensional geological shape (or a geo-body). The body can also be created manually or by using polygons.

Tsepav, 2022

Crossline dip: Dip in the direction of the Crossline axis, or in the direction of increasing crosslines.

Element: An element is a sub-division of various items (of the tree) that are displayed in a 3D scene. Inline, crossline, timeslices, horizon, wells etc are some elements. Each element is sub-divided into a sub-element. For instance an inline element can have further sub-elements e.g. inline at 120 that can contain up to eight different attributes.

Fault Stickset: The faults are interpreted on a section as a stick, and all sticks that belong to one fault are grouped in one sticksets. Therefore, a fault stickset contains an unordered collection of the interpreted sticks.

Inline dip: Dip in the direction of the Inline axis, or in the direction of increasing inline numbers.

Meta attribute: A meta-attribute is an attribute created from multiple input attributes. It is created either through neural networks, or through mathematical manipulations and/or logical operations.

Pickset: A Pickset is a collection of picked locations, i.e. inline-crossline-Z information. Picksets are part of a Pickset Group. For example a Pickset Group containing picks at fault locations may consist of different fault Picksets to differentiate between large faults and small faults, or to reflect picks on different inlines.

Pickset group: A Pickset group is a collection of different Picksets. Usually Picksets are grouped because they refer to the same object, e.g. Chimney_yes or Chimney_no.

Surface Data: It refers to a stored attribute grid in a horizon. An attribute is calculated on-the-fly or it can be calculated in a batch process.

Tree: The tree is the docking window, which is detachable and movable. This is used to display the data into a scene. The tree is attached to a scene and is labeled as *Tree Scene 1*. Where '1'

is the scene number. Each tree has its own elements that are displayed in corresponding scene.

Volren: A volren is a small 3D-cube loaded inside a sub-volume. It is an excellent tool for multi-volume rendering.

Directive attributes, filters, and Neural Networks, combined with modern visualization techniques, enable users to disclose information which remains hidden using conventional methods. These plugins deliver extra functionality to OpendTect:

- **The Horizon Cube:** This plugin auto-tracks a dense set of horizons (e.g. a horizon every 4ms). The Horizon Cube impacts all aspects of seismic interpretation work and allows the interpreter to extract more geology from the data. The HorizonCube is used for: detailed geologic model building, improving seismic inversion, sequence stratigraphic interpretation (SSIS) and correlating wells (new Well Correlation Panel).
- **The Well Correlation Panel:** New plugin to pick well log markers and correlate wells along (random) seismic tracks. In combination with the HorizonCube the Well Correlation Panel supports a HorizonCube slider for detailed seismic-steered correlations.
- **Steering:** attributes and filters are calculated along user-driven or data-driven directions.
- **SSIS (Sequence Stratigraphy Interpretation System)**
- **PSDM-VMB:** PSDM and VMB are new plugins. The VMB supports vertical update and horizontal based modules for velocity picking. The PSDM plug-ins supports Tomography, Kirchhoff migration, and a processing job builder.
- **CCB: Common Contour Binning** is used to detect subtle hydrocarbon-related seismic anomalies and to pin-point gas-water, gas-oil, and oil-water interfaces. CCB uses the power of stacking to enhance such anomalies. If all traces are stacked along the same contour line,

Tsepav, 2022

we can expect the hydrocarbon effect to stack up while stratigraphic variations and random noise will be canceled out.

- **MPSI:** This technology is considered the fastest stochastic inversion scheme currently on the market. MPSI is implemented as a series of five attributes in OpendTect's attribute engine. The attributes include: *Model builder*, *Error grid*, *Deterministic inversion*, *Stochastic inversion*, and *utilities*
- **Neural Network analysis:** Both supervised and unsupervised neural networks allow generation of meta attribute volumes that highlight any object of interest (Chimney, Salt, Faults, etc.).

2D Viewer

The 2D Viewer is used for examining the seismic data of an inline, crossline, or 2D lines in a 2D-screen. The seismic data can be viewed in two manners, namely "Wiggles" and "Variable Density" (VD). An example of a 2D view is shown in Figure 8

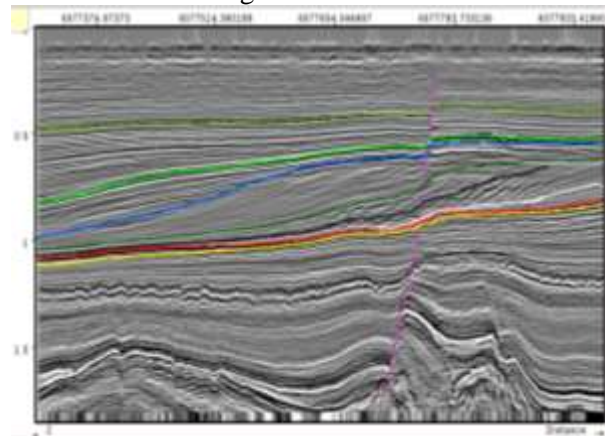


Figure 8: 2D data inline view in variable density (OpendTect 2010)

Interpreting Faults

The programme can be used to interpret faults (see Figure 9a and 9b) by using the following:

- **Add Attributes:** The selected attribute would be displayed on fault plane. It can be the original seismic, calculated attributes or others. Up to eight (8) attributes can be inserted for one fault.
- **Show histogram:** The histogram of the faults attribute can be displayed using this option. This allows the user to clip the range of a displayed attribute
- **Properties:** The option allows to change the general material properties for fault i.e. color, reflectivity, and transparency.
- **Use single color:** To display a fault plane in single color.
- **Display:** Three display modes for faults are categorized in the tree: 3D, *Fault sticks* or faults only at sections (inline/crossline).

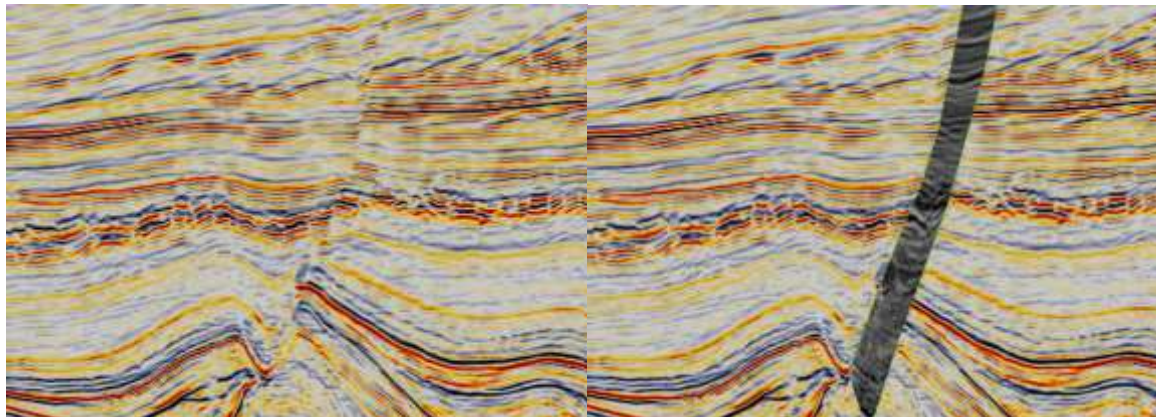


Figure 9: (a) Original Seismic data (b) Identified fault shown on the map

Horizon

Figure 10 (a) shows a horizon indicated from west to east. The program can:

Calculate isopach: This option computes the time or depth difference between two horizons. The computed grid will be displayed as a new layer on this horizon and may be stored as a surface data. The output will always be in seconds, meters, or feet.

Write Flattened Cube: It creates the flattened seismic at specified time value of horizon. The output is stored as a new flattened cube. The user can choose the benefit of this option by flattening the cube at the horizon.

Create flattened scene: This option enables the user to create a second scene in which the data is displayed relative to the flattened horizon. By flattening a horizon, the user gets an idea of the approximate section at the time of the deposition of this horizon. The tectonic history can be derived from the difference between the original section and the "restored" section. Another advantage of flattening the horizon is that it becomes easier to evaluate the depositional environments.

Track horizons: The Tracking pop-up menu is used to enable horizon tracking for the selected horizon (Figure 10b).

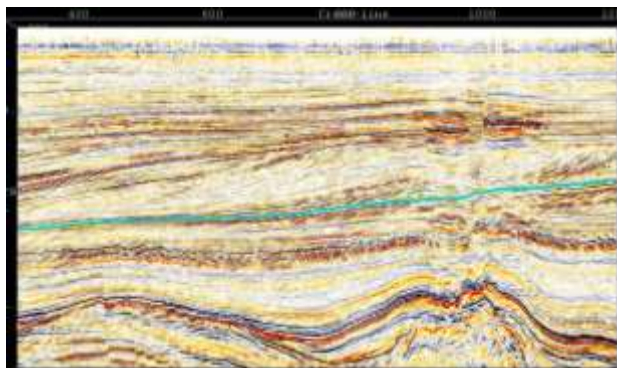
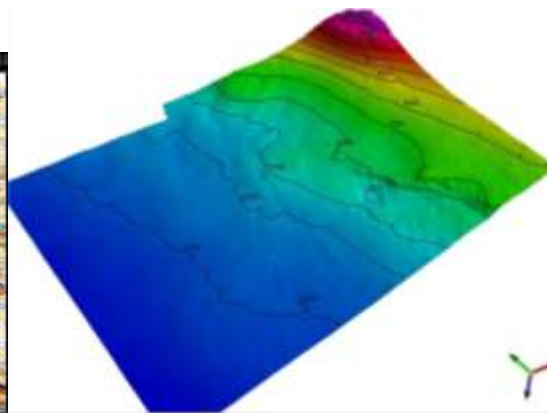


Figure 10: (a) Example of a horizon



(b) tracking for the selected horizon

Similarity

This is a multi-trace attribute that returns trace-to-trace similarity properties. Similarity is a form of "coherency" that expresses how much

two or more trace segments look alike. A similarity of 1 means the trace segments are completely identical in waveform and

Tsepav, 2022

amplitude. A similarity of 0 means they are completely dis-similar.

In OpendTect, we favor a different approach. We first try to find the direction of best match at every position, which is a result by itself: the dip. By using this dip we can then calculate the best Similarity between adjacent traces. Similarity is based on fundamental mathematics: the samples of the trace are seen as components of a vector, and the Similarity is defined in terms of distance in hyperspace.

The point about using the Similarity is that it's mathematically simple; it is very clear what is going on. Then, by combining different kinds of similarities and other attributes, you can always get much better results with lots less computing time.

Spectral decomposition

Spectral decomposition is a frequency attribute that returns the amplitude spectrum or wavelet coefficients. It unravels the seismic signal into its constituent frequencies, which allows the user to see phase and amplitude tuned to specific wavelengths. The amplitude component excels at quantifying thickness variability and detecting lateral discontinuities while the phase component detects lateral discontinuities. It is a useful tool for "below resolution" seismic interpretation, sand thickness estimation, and enhancing channel structures. The user can choose between two types of transform:

FFT: the Fast Fourier Transform. The FFT requires a short window (time-gate) and a step-size between the analyzed frequencies. This step can be interpreted as the frequency resolution.

In FFT only, the signal within the time-window will be transformed into frequency domain. The given step determines the output resolution, if necessary zeros will be added to acquire this resolution. The amplitude spectrum is calculated for the requested frequency. The time-window slides from top to bottom to cover the complete signal. In an ideal situation, the time-window encompasses one seismic event, which may be a superposition of multiple geological events which interfere in the seismic trace.

CWT: the Continuous Wavelet Transform. The CWT requires a wavelet type, *Morlet*, *Gaussian* or *Mexican Hat*

The CWT is defined as the sum over the signal multiplied by a scaled and shifted wavelet. The wavelet is shifted along the signal and at each position the correlation of the wavelet with the signal is calculated. The result is called a wavelet coefficient. The given frequency corresponds to the central wavelet frequency. The step determines the output resolution which is especially interesting when evaluating this attribute. Figure 11 shows the Spectral Decomposition (CWT) applied to a horizon.

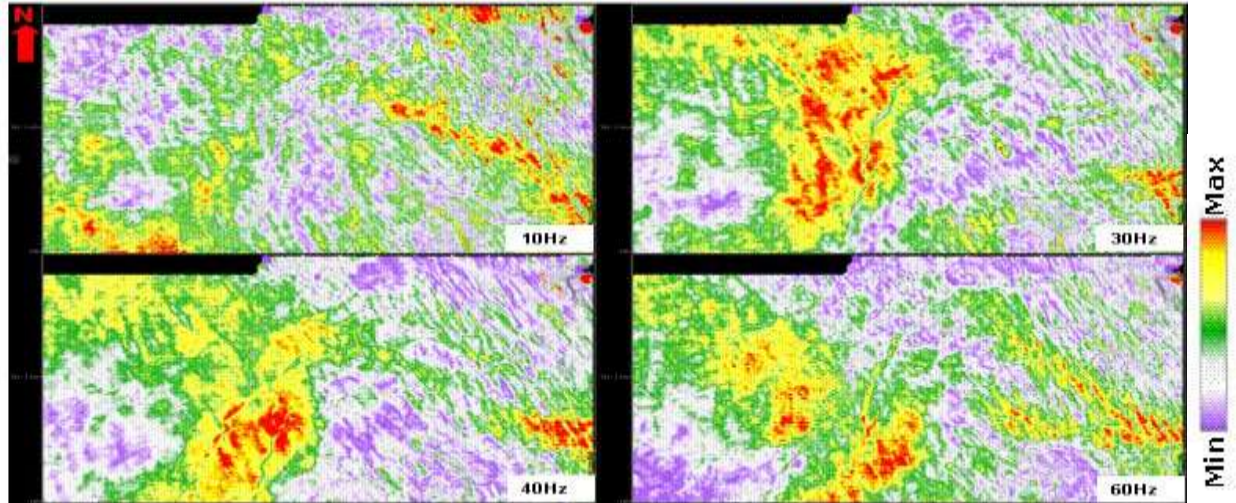


Figure 11: Spectral Decomposition (CWT) applied to a horizon. Notice that each index frequency is describing the specific parts of channels (NNE-SSW oriented). Also thinner and thicker parts of horizon along channels are highlighted clearly.

Time-frequency spectrum

The output frequency is best determined using the time-frequency spectrum panel. This panel displays the spectral decomposition output for all frequencies between 0Hz. and the Nyquist frequency of the data, computed with a step of 1Hz.

The time-frequency is then displayed in a 2D panel as shown in Figure 12

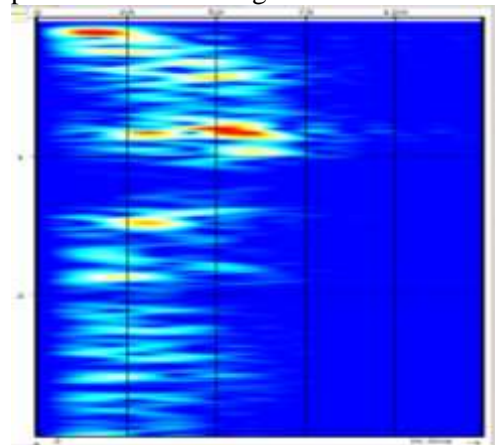


Figure 12: Time- Frequency Spectrum (OpenTect 2010)

Color blended display:

The RGBA- Red, Green, Blue, Alpha-channel (RGBA) blending attribute display is used to

create a normalized color-blended display that often shows features with greater clarity and enhances a detail map view. Traditionally, it is used to blend the iso-frequency responses (Spectral Decomposition), but a user can blend three/four different attributes that define a spectrum that is comparable. For instance, spectral decomposition outputs the amplitude at discrete frequencies. So, it renders the same output (unit=amplitude). Depending upon a geological condition or the objective, FFT short window or CWT (continuous wavelet transform) can be chosen. Results are best displayed on time/horizon slices and volume.

Figure 13 shows a coherency map (left) and a color blended map view (image on right) of the spectral decomposition. On the map, the yellowish colored fault boulder region is thicker as compared to the surrounding regions. The faults throw (red-color) are also clearly observable. Coherency or similarity, together with color blended spectral images can reveal better geological information.

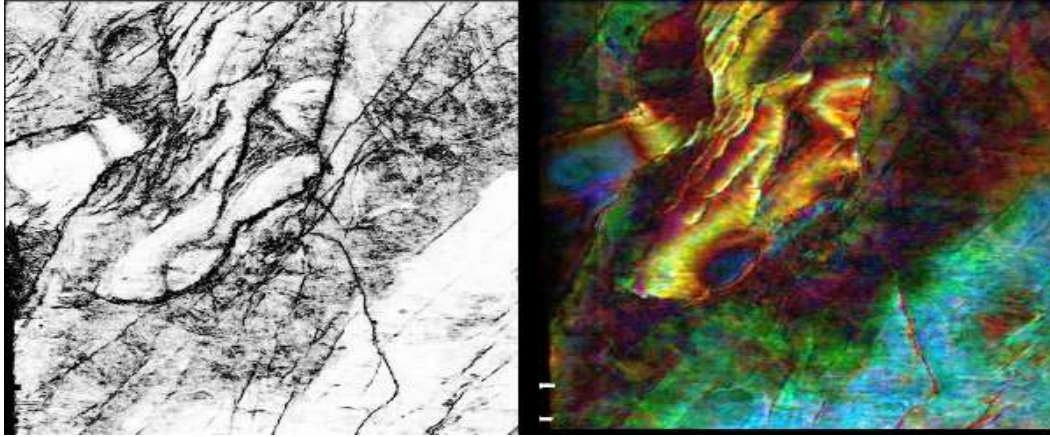


Figure 13: A color blended map view (image on right) of the spectral decomposition (red-10 Hz, green-20Hz, blue-40 Hz). Compare the results with the coherency map (image on left).

Frequency Filter—This attribute returns filtered data using FFT or Butterworth filter types (Figure 14). Input Data is bandpass filtered with the commonly used Fast Fourier Transform or Butterworth filter.

The difference between using the FFT or Butterworth filtering method is that, for the FFT, one considers the complete trace while for the Butterworth filter, only a "small" segment, depending on the selected number of poles, is taken into account. Using the Butterworth Filter results in a small shift in the seismic data.

The Filter type is set to Low Pass, High Pass or Band Pass based on its discriminating tendency against frequencies above or below a certain limiting frequency or outside of a given band of frequencies. The top frequency tapering applied to the extracted data in the time domain.

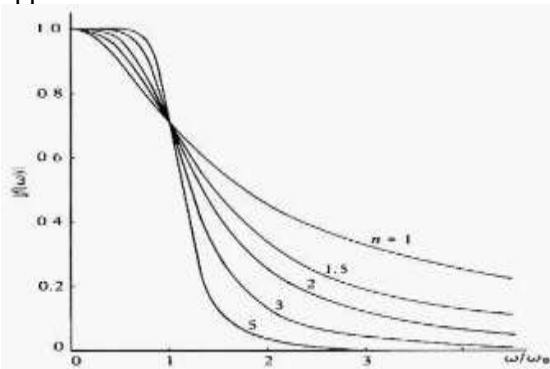


Figure 14: The curves of the Butterworth filter for various numbers of poles

CONCLUSION

Seismic reflection and refraction methods are two of the most commonly used geophysical methods in exploring the earth's crust and its sedimentary cover. Their relatively high structural resolution capacity and accuracy in data analysis, serve as their greatest advantages making them the rallying point for other geophysical methods. The methods have found effective use in mineral exploration, hydrocarbon exploration, groundwater development, geotechnical hazard and academic research purposes.

In this paper, the seismic refraction and reflection methods were reviewed. Derivations for various parameters such as depth to reflector, time of travel, critical distance, formation velocity etc. for reflective and refractive seismics have been derived. Methods of data acquisition, processing and interpretation have also been explained.

OpendTech, a dGB Earth Sciences software, for seismic post-processing and interpretation system, as well as a research and development platform for developing innovative seismic interpretation tools, was studied. The programme processes and displays data in 2D and 3D formats, interprets and displays faults, brings out and tracks horizons, evaluates similarity and carries out spectral decomposition of seismic data among many other uses. The package is loaded and has been shown to be an effective tool for seismic data processing and interpretation.

Tsepav, 2022

References

- Christian Heubschera and Karsten Gohl (2007). Reflection/Refraction Seismology. *Encyclopedia of Marine Geosciences* DOI 10.1007/978-94-007-6644-0_128-1, Springer Science + Business Media Dordrecht
- Eaton, D., Milkereit, B., and Salisbury, M., 2003, Hardrock seismic exploration; Mature technologies adapted to new exploration targets, in Eaton, D, Milkereit, B, and Salisbury, M., eds., *Hardrock Seismic Exploration: Society of Exploration Geophysicists, Geophysical Development Series*, v. 10, p. 1-6.
- Everhard Muijzert, Kenneth Welker, Iain Cooper, Simon Bittleston, Leendert Combee, Robert Ross, Edward Kotochigov (2015). *Marine Seismic Survey Systems and Methods Using Autonomously or Remotely Operated Vehicles*, Patent Publication number: 20150198731, Publication number: 20150198731
- Kennett Brian (2009). *Seismic Wave Propagation in Stratified Media*. Published by ANU E Press. The Australian National University Canberra ACT 0200, Australia, pgs 298. available online at: http://epress.anu.edu.au/seismic_citation.htm
- OpendTect (2010): *Seismic Interpretation Software*, version 4.6. dGB Beheer B.V. The license agreement is available at: <ftp://ftp.opendtect.org/pub/rel/LICENSE.txt>
- Parasnis D.S. (1979) *Seismic methods*. In: *Principles of Applied Geophysics*. Springer, Dordrecht. https://doi.org/10.1007/978-94-009-5814-2_7
- Salisbury, M., and Snyder, D., (2007). Application of seismic methods to mineral exploration, in Goodfellow, W.D., ed., *Mineral Deposits of Canada: A Synthesis of Major Deposit-Types, District Metallogeny, the Evolution of Geological Provinces, and Exploration Methods: Geological Association of Canada, Mineral Deposits Division, Special Publication No. 5*, p. 971-982.
- Talagapu Kiran Kumar (2017). *2D and 3D Land Seismic Data Acquisition and Seismic Data Processing* M.Sc.(Tech.) Geophysics Department of Geophysics College of Science and Technology Andhra University Visakhaptanam - 530003 Andhra Pradesh, India, pgs 116.
- Vlastislav Červený, Luděk Klimeš, Ivan Pšenčík (2007). *Seismic ray method: Recent developments*, Ed(s): Ru-Shan Wu, Valerie Maupin, Renata Dmowska, *Advances in Geophysics*, Elsevier, Volume 48, Pages 1-126, [https://doi.org/10.1016/S0065-2687\(06\)48001-8](https://doi.org/10.1016/S0065-2687(06)48001-8).
- Yilmaz, O., 1987, *Seismic Data Processing: Investigations in Geophysics*, No. 2, Society of Exploration Geophysicists, Tulsa, Oklahoma, 516 p.